

Vortex dynamics in $\text{YBa}_2\text{Cu}_3\text{O}_{7-\delta}$ superconducting films: Experimental evidence for an instability in the vortex system at high current densities

Z. L. Xiao

*Fakultät für Physik, Universität Konstanz, D-78434 Konstanz, Germany
and Department of Materials Science, Sichuan Union University, Chengdu 610064, China*

P. Ziemann

*Fakultät für Physik, Universität Konstanz, D-78434 Konstanz, Germany
and Abteilung für Festkörperphysik, Universität Ulm, D-89069 Ulm, Germany*

(Received 2 October 1995; revised manuscript received 11 December 1995)

Current-voltage characteristics and the temperature dependence of the electrical resistivity of $\text{YBa}_2\text{Cu}_3\text{O}_{7-\delta}$ thin films were investigated in magnetic fields up to 5 T. For a given magnetic field, both voltage and resistivity jumps could be observed at high driving forces when the current density and the temperature reached the critical values J^* and T^* , respectively. Excellent scaling of the experimental data was obtained by describing the field and temperature dependence by $J^*(H, T) = J^*(T)/(1 + H/H_0)^\alpha$ and $J^*(T) \sim (1 - T/T_{c0})^{3/2}$ with $1/3 \leq \alpha \leq 3/4$ and H_0 and T_{c0} being constants. These results indicate a well-defined vortex instability closely resembling that predicted by Larkin and Ovchinnikov (LO) for high flux flow velocities. In the present case, however, by referring to the current-voltage (I - V) characteristics, this instability can be demonstrated to occur even at temperatures well below T_g defined by separating negatively from positively curved I - V characteristics. Analyzing the experimentally observed instability according to LO theory, the temperature dependence of the inelastic quasiparticle scattering time has been obtained. As a new aspect, the corresponding critical flux-flow velocity exhibits a significant field dependence for small magnetic fields, while for fields above 2 T this dependence seems to disappear. [S0163-1829(96)02622-7]

I. INTRODUCTION

The issue of vortex dynamics in high- T_c superconductors is both of practical and fundamental interest. Thus, many theoretical as well as experimental studies have addressed this topic during the last years and new, in some cases unexpected, behavior has been reported. Especially interesting in the present context are the suggested new phases and phase transitions of the vortex system like the vortex glass and its transition into the melt. Of similar importance is the distinction between different dissipation regimes like flux creep as described, e.g., by the model of collective creep, or thermally activated flux flow (TAFF) and flux flow (FF), each regime exhibiting a specific signature in current-voltage (I - V) characteristics. Recent reviews on this very active field of research are given in Refs. 1 and 2.

For high-driving forces, a characteristic instability of the vortex dynamics has been predicted by Larkin and Ovchinnikov (LO) many years ago³ leading to a discontinuous voltage jump in the I - V curves at a critical value I^* . The underlying idea is that the viscous friction, which a vortex experiences during its movement, is a nonmonotonic function of the velocity with a maximum at a critical value. Above this critical velocity, the viscosity coefficient decreases leading to an even higher velocity and so on so forth giving rise to the above instability. Experimentally, this phenomenon has been studied for a number of low- T_c superconductors and reasonable agreement with LO theory has been found.^{4,5} Corresponding experiments on high- T_c superconducting films were reported only recently⁶ and interpreted in

terms of LO theory providing information on the inelastic-scattering time of quasiparticles. The applicability of such an interpretation is not obvious, since the experimentally observed voltage jumps could also be due to alternative mechanisms like depairing,^{7,8} Josephson behavior,⁹ or, as proposed recently, vortex system crystallization.¹⁰

To clarify this situation, we have repeated and extended the work of Doettinger *et al.*⁶ by studying the behavior of $\text{YBa}_2\text{Cu}_3\text{O}_{7-\delta}$ thin films grown on different substrates. Additional new insight could be provided by determining complete sets of current-voltage characteristics at different temperatures and magnetic fields rather than just concentrating on the voltage jumps. In this way, it could be tested whether the occurrence of the instability is restricted to a certain dissipation regime like, e.g., flux flow. In addition, by measuring electrical resistance at different temperatures (R - T) and magnetic fields applying a wide range of currents, a second independent set of data was obtained and could be checked for consistency.

II. EXPERIMENTAL DETAILS

$\text{YBa}_2\text{Cu}_3\text{O}_{7-\delta}$ thin films with different thickness were deposited by sputtering on (100) oriented SrTiO_3 substrates¹¹ and by evaporation onto sapphire substrates with CeO_2 buffer layers.¹² As revealed by x-ray analysis, all films were purely c -axis oriented with rocking angles as determined on the (005) reflexes below 0.5° . After patterning as bridges (length 100 or 500 μm , width 5 or 10 μm) by photolithography and wet chemical etching, Ag contact pads were evaporated allowing the measurement of R - T and I - V

TABLE I. Sample parameters.

Sample	Substrates	Thickness (nm)	Bridge width (μm)	Bridge length (μm)	RRR ($R_{300\text{K}}/R_{100\text{K}}$)	$\rho_{100\text{K}}$ ($\mu\Omega\text{ cm}$)	$T_c(R=0)$ ^a (K)
A	CeO ₂ /Al ₂ O ₃	250	5	100	2.82	107.38	87.20
B	CeO ₂ /Al ₂ O ₃	250	10	100	2.72	138.60	85.60
C	CeO ₂ /Al ₂ O ₃	300	5	100	2.80	100.06	87.00
D	SrTiO ₃	200	10	500	2.62	136.40	84.80 ^b
E	SrTiO ₃	200	10	500	3.03	87.40	87.70
F	SrTiO ₃	50	10	500	2.77	80.90	90.50

^aMeasured at low current limit without external magnetic field.

^bAfter $10^{14}/\text{cm}^2$ He⁺ irradiation.

curves using the standard four-point method. In addition, external magnetic fields up to 5 T could be applied. In the present study, in all cases these fields were oriented parallel to the c axis of the films. In total, we have studied six samples, three on both types of substrates. All of them showed similar results. Their zero-resistance temperatures measured in the low current density limit ($I \leq 10 \mu\text{A}$) without external magnetic field ranged between 84.80 and 90.50 K with residual resistance ratios (RRR) ($=R_{300\text{K}}/R_{100\text{K}}$) between 2.62 and 3.03. The important sample parameters are summarized in Table I. In the following, we will concentrate on the results obtained for sample A, a YBCO bridge (100 μm long, 5 μm wide, and 250 nm thick) prepared on sapphire.

A crucial point in the present experiments is the avoidance of excessive Joule heating possibly occurring in the film as well as in the electrical contacts (typical resistance 0.2 Ω) due to the high current densities. In the present case, the YBCO films were fixed with vacuum grease onto a copper sample holder mounted within vacuum at the bottom of a 1He-/1N₂ cryostat. The current through the film was varied either by using rectangular pulses (with a typical current-on time of 1.5 s followed by intervals without current of typically 3 s) or by applying a triangular ramp increasing the current up to the voltage jump and then switching it off. In both cases, the maximum voltage drop along the bridge was limited to 1 V and the maximum current to 100 mA, respectively, in order to protect the bridge from destruction. For both experimental procedures and for SrTiO₃ as well as for sapphire substrates, no thermal hysteresis of the current-voltage characteristics below J^* has been observed indicating that excessive Joule heating can be excluded. A small shift, however, of the film temperature relative to the constant temperature of the thermometer caused by the applied current has to be expected, the magnitude of which can be estimated as follows. Assuming the experimentally determined thermal boundary resistances for YBaCuO films on different substrates as reported in Refs. 13 and 14 (typical values are $10^{-3} \text{ cm}^2 \text{ K W}^{-1}$ on sapphire, $10^{-4} \text{ cm}^2 \text{ K W}^{-1}$ on SrTiO₃), the estimated temperature shifts due to the maximum heating powers just below the observed voltage jumps are 1.2 K for the YBaCuO bridges on sapphire and 0.02 K for the larger bridges on SrTiO₃ substrates (cf. Table I), respectively. To experimentally corroborate these estimates additional I - V curves in external fields up to 0.8 T were determined on sample D (YBaCuO on SrTiO₃) by immersing the bridge directly into liquid nitrogen (77 K). The

resulting I - V characteristic is slightly shifted towards higher currents as compared to the results obtained for this sample mounted under vacuum. Attributing this shift to different effective bridge temperatures in both experiments, from the known temperature dependence of the I - V curves a difference of 0.24 K can be calculated. Though larger than the above estimate based on literature values for the heat resistance, the experimentally observed heating effect is too small to have any significant bearing on the major conclusions of the present work. Especially, it can be excluded that the reported phenomenon of voltage jumps itself is caused by heating. Rather, the unavoidable slight shifts in temperature lead just to small changes of the corresponding critical values J^* by typically 5%.

III. RESULTS AND DISCUSSION

A. Jumps in current-voltage characteristics

1. Temperature and magnetic field behavior

In Fig. 1(a), current-voltage characteristics are presented, which were taken in an external magnetic field of 2 T at different temperatures as assigned to each curve. For $T < 80$ K well-defined voltage jumps (experimentally limited to a maximum of 1 V) can be observed at temperature-dependent critical current densities $J^*(T)$. For temperatures closer to T_c , these voltage jumps disappear. For a direct comparison to earlier data on the conventional superconductors Al,^{4,5} In,^{4,5} and Nb,¹⁵ in Fig.1(b) the YBCO characteristics are shown for different external magnetic fields as assigned to each curve determined at the fixed temperature 77 K. Clearly, the critical current densities J^* , where the voltage jumps occur are shifted to lower values by increasing magnetic fields, the I - V curves become more smeared and eventually, at high fields the jumps disappear. This behavior is similar to what has been found for the above conventional superconductors.

The observed results allow to exclude the possibility to attribute the voltage jumps to the phenomenon of a vortex system crystallization. In this case, the critical current density J^* is expected to be shifted to higher values by increasing the temperature.¹⁰ Also, the shape of the I - V curves reported here is not consistent with that expected for Josephson junctions.^{7,9} Thus, an interpretation in terms of the LO instability model³ appears to be appropriate, though in this model, external magnetic fields small compared to the upper critical field H_{c2} should not affect the voltage instability. Before

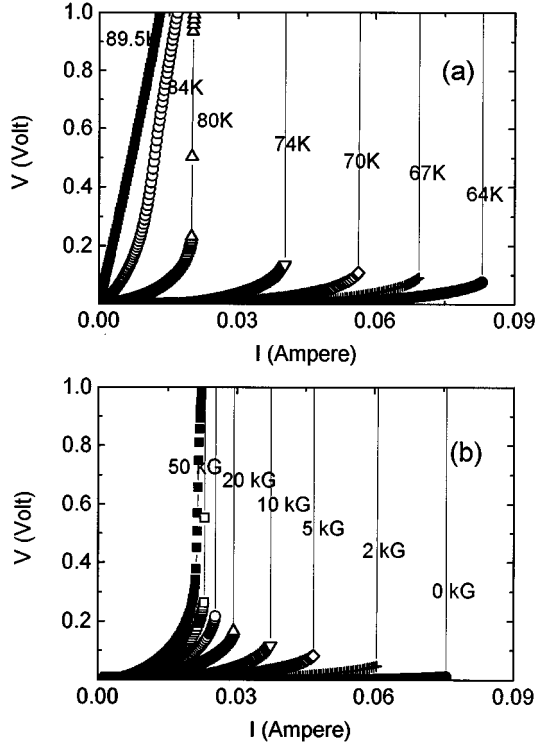


FIG. 1. Current-voltage characteristics of a $\text{YBa}_2\text{Cu}_3\text{O}_{7-\delta}$ bridge (sample A): (a) isotherms at temperatures as assigned to each curve in a magnetic field of 20 kG; (b) 77 K isotherms in different magnetic fields as assigned to each curve. The solid lines indicate the voltage instability, which was experimentally limited to 1 V.

applying the LO model to the above results, in the following the magnetic field and temperature dependence of the critical current density $J^*(H, T)$ will be analyzed in terms of a generalized critical state model.

Extending the models of Beam,¹⁶ Anderson and Kim,¹⁷ as well as of Irie and Yamafuji,¹⁸ a generalized critical state model has been developed recently by Xu *et al.*¹⁹ There, the temperature and magnetic-field dependence of the critical current density defined by one of the standard voltage or electrical field criteria, is separated and expressed as

$$J_c(H, T) = J_c(T) / (1 + H/H_0)^\alpha, \quad (1)$$

where α is a constant exponent and $J_c(T)$ is a function describing the temperature dependence. Equation (1) delivers the Bean form for $\alpha=0$ and the Anderson-Kim form for $\alpha=1$. If $H/H_0 \gg 1$, the Irie form is obtained. Calculations of the magnetic-field dependence of the magnetization based on the above generalized critical state model showed good agreement with experimental data.²⁰ Also the application of this model to analyze the experimentally observed magnetic field dependence of the transport critical current density in polycrystalline $\text{YBa}_2\text{Cu}_3\text{O}_{7-\delta}$ samples resulted in a consistent description.²¹ In the following, we apply the separation ansatz of Eq. (1) to model the field and temperature behavior of the critical current density $J^*(H, T)$ related to the observed voltage instability.

In Fig. 2 the experimental data are presented, which were used for the analysis of $J^*(H, T)$. In the upper Fig. 2(a), the

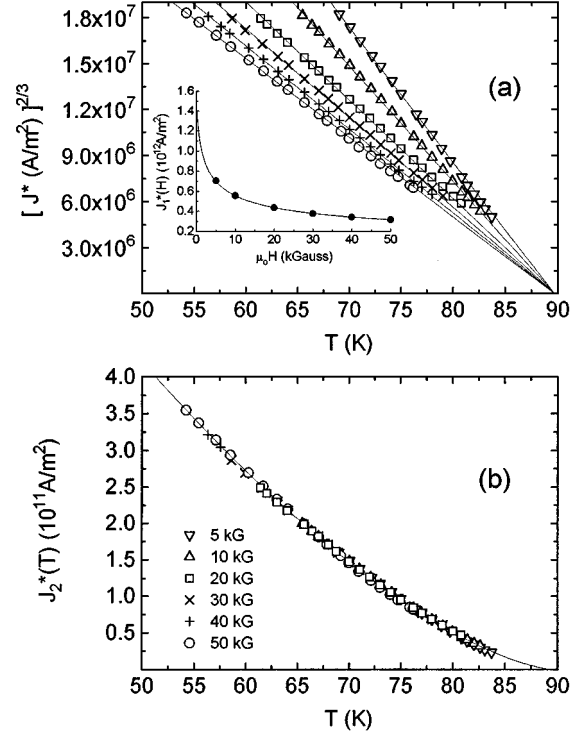


FIG. 2. Temperature dependence of the critical current density J^* resulting in the voltage instability: (a) In different magnetic fields $\mu_0 H = 5, 10, 20, 30, 40,$ and 50 kG from right to left [same symbols as defined in (b)]. The solid lines are fits of Eq. (2) to the data with $T_{c0} = 89.70$ K, $\alpha = 0.3643$, $\mu_0 H_0 = 801$ G, and $J^*(0, 0) = 1.44 \times 10^{12}$ A/m² as well as field-dependent values $J_1^*(H)$, which are given in the inset as solid dots. The solid line through these dots is obtained from $J_1^*(H) = A / (1 + H/H_0)^\alpha$ with the same parameters as above. (b) Temperature-dependent part $J_2^*(T)$ as defined in Eq. (2) scaling the field dependence according to $J_1^*(H)$ with the parameters given above. The solid curve is calculated from Eq. (2) using still the same set of parameters. [Symbols in (a) and (b) are identical.]

temperature dependence of the critical current density is given for different magnetic fields ranging from 5 to 50 kG and the results are plotted in the form $J^{*2/3}$ vs T . Correspondingly, the solid lines through the data are fits to the expression

$$\begin{aligned} J^*(H, T) &= J_1^*(H) (1 - T/T_{c0})^{3/2} = J_2^*(T) / (1 + H/H_0)^\alpha \\ &= [A / (1 + H/H_0)^\alpha] (1 - T/T_{c0})^{3/2}, \end{aligned} \quad (2)$$

where the constant A can be identified with $A = J^*(H=0, T=0)$ and T_{c0}, H_0, α are fit parameters. Clearly, Eq. (2) together with the derived numerical values $\alpha = 0.3643$, $T_{c0} = 89.70$ K, $\mu_0 H_0 = 801$ G, and $J^*(0, 0) = 1.44 \times 10^{12}$ A/m² provides an excellent description of the experimental results. Each of the fits presented in Fig. 2(a) delivers a value $J_1^*(H)$. These values are given as solid dots in the inset of Fig. 2(a), while the solid line through all these points represents the field-dependent part of Eq. (2) corresponding to the above parameters. This good agreement demonstrates the self-consistency of the different ways analyzing the experimental data. The separation ansatz of Eq. (2) should also allow one to plot the temperature dependence

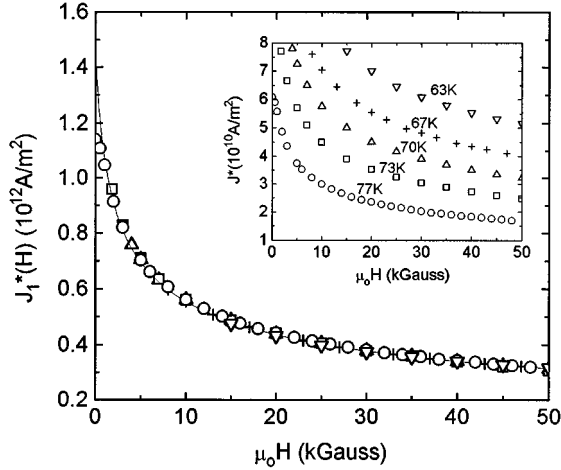


FIG. 3. Field dependence $J_1^*(H)$ of the critical current density leading to the voltage instability as derived from the measurements shown in the inset taken at the different temperatures assigned to each curve. The data points are obtained by temperature scaling according to Eq. (2) using the same parameters as used in Fig. 2. These parameters also result in the solid line if Eq. (2) is applied giving the same curve as in the inset of Fig. 2.

of the J^* data corresponding to different magnetic fields onto one common $J_2^*(T)$ curve. This is tested in Fig. 2(b), where the symbols represent the experimental results for different magnetic fields and the solid line is calculated from Eq. (2) using the same parameters as given above. As can be seen, the result of this test confirms that Eq. (2) excellently describes the field and temperature dependence of the critical current density J^* related to the voltage instability.

Since the description of the temperature dependence by a power law with exponent $3/2$ is quite commonly found for depinning and/or depairing critical current densities J_c , it is tempting to interpret the voltage jump at J^* as a depinning instability rather than in terms of the LO model. In the latter model, however, the temperature dependence of J^* results from different temperature-dependent contributions like the inelastic-scattering time of quasiparticles [cf. Eq. (3)] and an overall description by a $3/2$ power law over a restricted regime cannot definitely be excluded. Here, a more decisive test is offered by the magnetic-field dependence expected for the different scenarios. While for depinning related phenomena, power laws as, e.g., given above by $J_1^*(H)$ have been reported previously,^{1,22} in the LO model J^* should be practically field independent.^{5,6} To test the field dependence, an additional set of experimental data were taken on the same film as above at different fixed temperatures applying much smaller H intervals than in Fig. 2. The corresponding results for J^* are given in the inset of Fig. 3. According to Eq. (2), all these data points should fall onto one common $J_1^*(H)$ curve after rescaling the temperature effect. This behavior is demonstrated in Fig. 3, where the rescaled data are plotted as a function of the magnetic field with the same symbols as in the inset, and the solid line represents $J_1^*(H)$ as defined in Eq. (2) using the above values of the fitting parameters A, H_0 , and α . Similar results were obtained for all films with α ranging between $1/3 \leq \alpha \leq 3/4$ depending on film thickness and quality. Thus, the data presented in Figs. 2 and 3 con-

vincingly demonstrate a significant field dependence of the ‘‘jump’’ current J^* in contrast to what is expected at least by the low field version of the LO theory. This may be taken as a strong hint that an additional depinning mechanism is involved in the observed voltage instability. On the other hand, such a field dependence has been observed also for conventional superconductors though the corresponding instability otherwise could consistently be described in terms of the LO model.⁵ Those authors already addressed this problem and mentioned that an extension of the LO theory to finite magnetic fields would be an interesting question. Obviously, the theoretical answer is still pending. With respect to YBCO films the authors of Ref. 6 report that J^* ‘‘remained approximately constant’’ during their variation of the magnetic field within the range $1 \leq B \leq 4$ T. Comparison to Fig. 3 shows that their statement is compatible with our findings, since within this field range the variation of J^* becomes small. It may be worth noting at this point that though J^* is monotonously decreasing for increasing magnetic fields, the corresponding Lorentz force density $F^* = J^*B$ ($B = \mu_0 H$) acting on the vortices is monotonously increasing.

2. Analysis according to LO theory

According to the Larkin-Ovchinnikov theory a voltage instability in the I - V characteristics is expected to occur whenever the vortex velocity reaches the critical value

$$v^* = \{D^{1/2} [14\zeta(3)]^{1/4} (1-t)^{1/4}\} / [\pi\tau_{in}]^{1/2}, \quad (3)$$

where $D = (v_f d)/3$ is the quasiparticle diffusion coefficient with the Fermi velocity of v_f and the electron mean free path d ; τ_{in} is the inelastic-scattering time of quasiparticles and $\zeta(3)$ is the Riemann ζ function of 3. The flux-flow voltage corresponding to the critical velocity is given by

$$V^* = v^* \mu_0 H L, \quad (4)$$

where L is the distance between the voltage probes, in our case it is given by the length of patterned bridge. Applying Eq. (4), the critical velocity v^* has been extracted for different temperatures and the results are presented in Fig. 4(a) as a function of the magnetic field. Similar to J^* , a clear field dependence is observed for v^* , which, however, systematically becomes smaller for increasing magnetic fields and decreasing temperatures. For example, at 77 K and high magnetic fields (>1.5 T), v^* is practically field independent [cf. Fig. 4(a)] as expected from LO theory. For lower temperatures or at high temperatures in combination with low magnetic fields, one finds that $v^* \sim H^\beta$ with $\beta = -(0.58 \pm 0.10)$ is a good approximation of the field dependence. As already mentioned, these observations are similar to those found for conventional superconductors and compatible with the previous results reported for YBCO.

Once the critical velocities are determined, the rate of inelastic quasiparticle scattering $1/\tau_{in}$ can be calculated from Eq. (3) for different temperatures, if appropriate values for the Fermi velocity and the mean free path are assumed. To allow a direct comparison, for these properties the same values were taken as in Ref. 6, i.e., $v_f = 1 \times 10^7$ cm/s and $d = 5$ nm. The corresponding results are shown in Fig. 4(b). Added to this figure are the previous results on YBCO films obtained by Doettinger *et al.*⁶ Taking into account the differ-

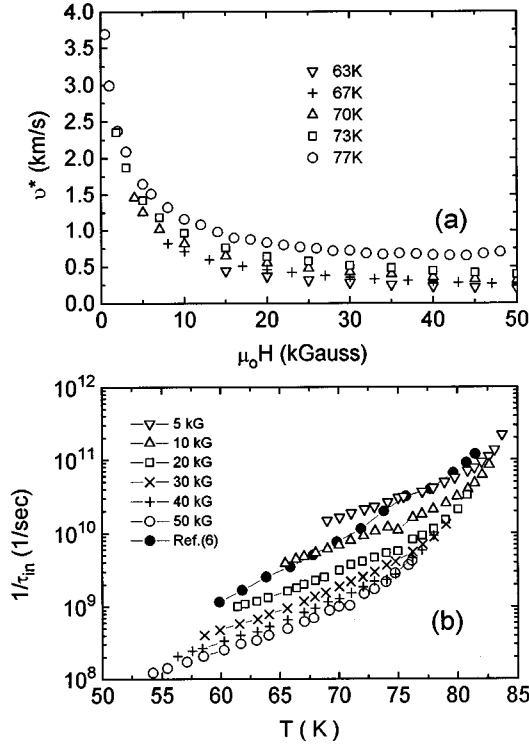


FIG. 4. (a) Magnetic field dependence of the critical flux-flow velocity v^* [cf. Eq. (4)] determined at different temperatures as assigned in the inset (same symbols as in Fig. 3). (b) Temperature dependence of the inelastic-scattering time according to Eq. (3) in different magnetic fields as given in the inset. The data from Ref. 6 are added for comparison.

ent preparation techniques probably leading to a variation of film qualities, the general behavior of the scattering rates exhibits a satisfying agreement. Especially, the present data confirm the relative steep decrease of $1/\tau_{in}$ if the temperature is lowered as opposed to what is found by microwave surface impedance measurements. As already argued in Ref. 6, this might be due to the fact that $1/\tau_{in}$ is dominated by inelastic rather than elastic processes and the voltage instability is exclusively related to flux-flow processes.

As a consequence of Eq. (3), the field dependence of the critical velocity as shown in Fig. 4(a) is immediately reflected in a corresponding field dependence of the scattering rate $1/\tau_{in}$ as can be seen from Fig. 4(b). Thus, this field dependence rather than being intrinsic, is probably an artifact due to the approximations of the theoretical description, which does not include finite magnetic fields. Here, further theoretical work appears necessary to account for the experimental observations.

As mentioned in Sec. II, great attention has been paid in avoiding effects due to Joule heating by applying the sample current either in a pulsed or in a continuous way and checking for thermal hysteresis. In the following, an additional independent set of data demonstrating the instability will be presented, which has been obtained by measuring the temperature dependence of the film resistance for different fixed current densities and magnetic fields.

B. Jumps in resistivity-temperature characteristics

In Fig. 5(a) the temperature dependence of the resistivity is plotted for the same YBCO film as above at different

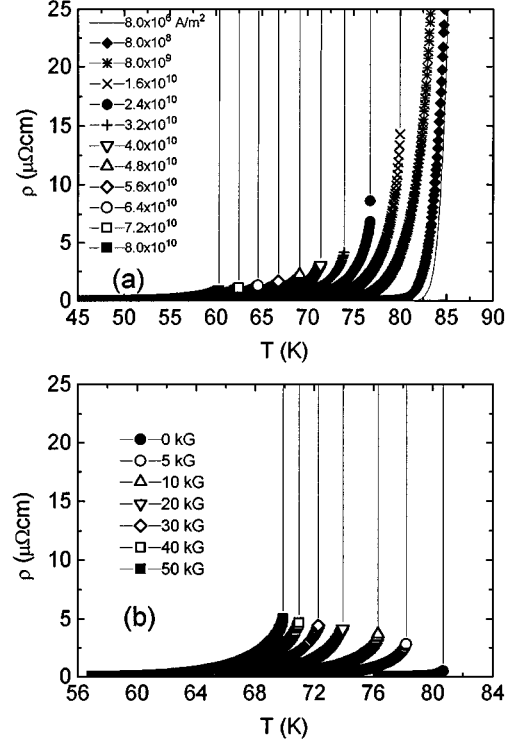


FIG. 5. Temperature dependence of the resistivity of a $\text{YBa}_2\text{Cu}_3\text{O}_{7-\delta}$ bridge (sample A as above): (a) In a constant magnetic field $\mu_0 H = 20 \text{ kG}$ and using different current densities as given in the inset; (b) at a constant current density $J = 3.2 \times 10^{10} \text{ A/m}^2$ ($I = 40 \text{ mA}$) in different magnetic fields as given in the inset.

applied current densities as indicated in the inset and at a constant magnetic field of 2 T. As expected from the results given in Sec. III A, whenever the applied current density J reaches the critical value $J^*(H)$ at a well-defined temperature $T = T^*$ related to the value of the fixed magnetic field H , a voltage instability occurs, which manifests itself as a resistivity jump in the present measurements. This resistivity jump becomes smaller and eventually disappears for decreasing current densities. In analogy to the I - V curves, where the voltage jumps defined a critical current density $J^*(H, T)$ depending on the external parameters H and T , the resistivity jumps allow to extract a critical temperature $T^*(H, J)$ now depending on the parameters H and J . Though in principal both types of measurements provide the same information, in practice only the $\rho(T)$ data allow a precise determination of $T^*(H)$, since otherwise I - V curves quasi-continuous in the parameters T and H would be needed. In Fig. 5(b), the field dependence of the critical temperature is demonstrated at a fixed current density of $3.2 \times 10^{10} \text{ A/cm}^2$ exhibiting a clear shift to lower temperatures for higher magnetic fields. Consistency of the data presented in Fig. 5 with those of the I - V curves can be checked in the following way. For a given current density J and magnetic field H , the temperature $T = T^*$ corresponding to the condition $J = J^*$ can be calculated from Eq. (2) resulting in

$$T^* = T_{c0} \{1 - [J/J_1^*(H)]^{2/3}\} \quad (5)$$

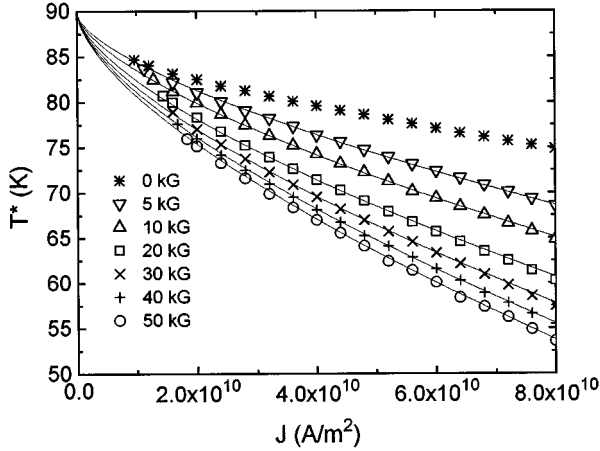


FIG. 6. The current dependence of the critical temperature T^* related to the voltage instability for different magnetic fields as indicated in the inset. The solid curves are calculated from Eq. (5) with the same values for $T_{c0}, H_0, J^*(0,0)$ and α as above.

with J_1^* and T_{c0} as defined above. The experimental data points $T^*(J)$ are given in Fig. 6 for the different magnetic fields indicated in the inset. Using identical values for the parameters $T_{c0}, H_0, J^*(0,0), \alpha$ as extracted from the I - V data of Fig. 2 and reported above, the solid lines in Fig. 6 have been calculated according to Eq. (5). The excellent agreement between the solid lines and the experimental data confirm the quantitative consistency of the independently obtained sets of results. Similarly, from the data of Fig. 5(b), the field dependence of the critical temperature T^* can be determined and the results are presented as H - T diagrams for different current densities J in Fig. 7. These diagrams closely resemble the irreversibility lines, which are generally observed for high- T_c superconductors and which very often exhibit a power-law behavior of the form $H \sim [1 - T/T_c(H=0)]^m$, where T_c stands for the transition temperature into the superconducting state. The irreversibil-

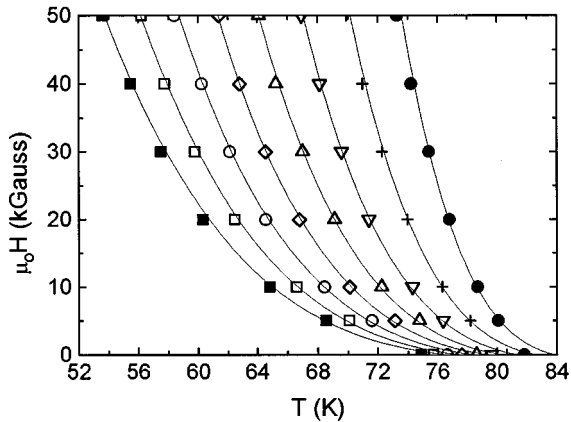


FIG. 7. Magnetic field dependence of the critical temperature $T^*(H$ - T diagram) for different current densities ranging from $2.4 \times 10^{10} \text{ A/m}^2$ (30 mA) at the right to $8.0 \times 10^{10} \text{ A/m}^2$ (100 mA) at the left in steps of $8 \times 10^9 \text{ A/m}^2$ (10 mA). The symbols are the same as in Fig. 5(a). The solid curves are calculated from Eq. (5) using $J_1^*(H)$ as extracted from Fig. 3 and the same parameters as above.

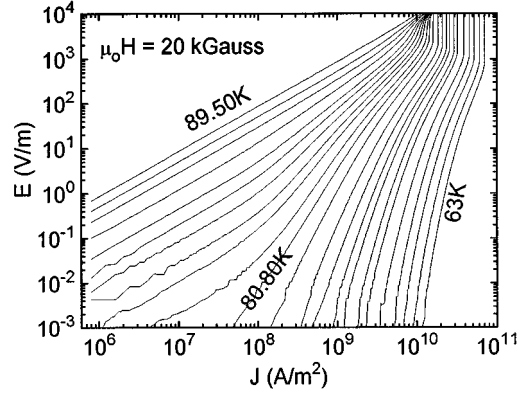


FIG. 8. Double-logarithmic plot of E - J isotherms determined on a $\text{YBa}_2\text{Cu}_3\text{O}_{7-\delta}$ bridge (sample A) in a magnetic field of 20 kG and for a temperature range between 63 and 89.50 K.

ity line has found various interpretations, e.g., as being due to a vortex glass transition,²³ to depinning,²⁴ or vortex lattice melting²⁵ and for the exponent m quite commonly a value of $m=3/2$ has been reported. In the present case, if such a power law is fitted to the data of Fig. 7, exponents within the range $1.60 \leq m \leq 2.30$ are extracted with a dependence on the current density. This range of m values is even enlarged to $1.30 \leq m \leq 2.50$, if the results for all different samples are included. On the other hand, Eq. (5) shows that in case $J_1^*(H)$ is known, the H - T diagrams can be calculated. Taking $J_1^*(H)$ as deduced from the I - V curves of Fig. 3 with the fit parameters as given above, this calculation has been performed and the corresponding results are included as solid lines in Fig. 7. Again, the excellent agreement between the calculation and the experimental data confirm the above-stated quantitative consistency of the two independent measurements.

C. Discussion and summary

Based on the reported experimental results, clear evidence could be provided for an instability of the vortex system in YBCO films at large Lorentz forces. Interpreting this phenomenon according to LO theory, the temperature dependence of the inelastic-scattering rate of quasiparticles could be extracted confirming recent experiments on the same material.⁶ On the other hand, the critical current density $J^*(H, T)$, where the instability is observed, exhibits a significant field dependence in contrast to the theoretical prediction. Furthermore, the separability as given by Eq. (2) with functions closely resembling the behavior of the standard critical current density $J_c(H, T)$, leads to the assumption that the specific vortex pinning present in the sample is somehow related to the voltage instability. This assumption is different from the premise of LO theory, where the voltage jump results as a consequence of a velocity-dependent damping coefficient within the flux-flow regime of the vortex system. Thus, it is of utmost importance to experimentally determine the dynamic situation of the vortex system just before the driving forces reach the critical value leading to the instability. This type of information is provided in Fig. 8, where E - J isotherms ranging from 63 K at the right to 89.50 K at the left, are presented on a double logarithmic scale as ob-

tained in a magnetic field of 2 T. Clearly, the almost linear E - J curve at $T_g = 80.80$ K separates the characteristics into two regimes with negative and positive curvatures, respectively. According to a widely accepted interpretation, for $T > T_g$ the almost linear part of an isotherm at low current densities is attributed to TAFF followed by the nonlinear creep part. For temperatures approaching T_c , ohmic behavior becomes dominating indicating flux flow as the governing process. For temperatures below T_g and at the lower end of current densities, the resulting positively curved isotherms are either attributed to a transition into the vortex glass state or are described by the model of collective creep. In the context of the present work, the most remarkable result visible in Fig. 8 is the occurrence of the voltage instability at high current densities for practically all isotherms independent of whether their temperature is above or below T_g . The sharpness of the corresponding electric-field-voltage jump, however, is decreasing for increasing temperatures.

The fact that the voltage instability does occur even below T_g if high enough current densities are applied, points to the following interpretation, which still preserves the basic idea of LO theory. At temperatures below T_g the specific dynamics of the vortex glass state allows relative high current densities to be applied before a preset voltage criterion is fulfilled, i.e., dissipation is strongly reduced. On the other hand, in the limit of large current densities, a vortex glass isotherm should eventually approach the ohmic flux-flow behavior. In the present case, however, it appears that at the critical value J^* , the corresponding driving force density J^*B is sufficient to impose the critical LO velocity v^* on the vortices before they enter the flux-flow regime. This implies the assumption, that independent of any specific vortex dynamics as, e.g.,

present in a vortex glass or during flux flow, if the critical LO velocity is enforced on the vortices by sufficiently large driving forces, the LO instability takes place. The value, however, of the necessary driving force or current density J^* , strongly depends on this specific dynamics immediately leading to a significant field and temperature dependence $J^*(H, T)$. Since the specific vortex dynamics is intimately related to the pinning behavior of a sample, it is plausible that the functional form of $J^*(H, T)$ closely resembles that of the standard critical current density $J_c(H, T)$, which is similarly related to pinning. On the other hand, for temperatures well above T_g , where the E - J characteristics of Fig. 8 exhibit an almost linear behavior, conventional LO theory should deliver a good description of the instability. This expected trend is confirmed, e.g., by the data presented in the inset of Fig. 3, which demonstrate that the critical current density J^* becomes more and more field independent, i.e., LO-like, for increasing magnetic fields.

Further work is in progress to test the influence of the field orientation relative to the c axis of the epitaxial films as well as of additional disorder introduced into the films by ion bombardment on the presently reported voltage-resistivity instability.

ACKNOWLEDGMENTS

We would like to thank Dr. Ch. Neumann for supplying us with films on sapphire substrates. The experimental advice and support by J. Häring, Ch. Heinzl, and Th. Theilig is gratefully acknowledged. One of us (Z.L.X.) was financially supported by the German Academic Exchange Service (DAAD).

-
- ¹G. Blatter, M. V. Feigel'man, V. B. Geshkenbein, A. I. Larkin, and V. M. Vinokur, *Rev. Mod. Phys.* **66**, 1125 (1994).
²E. H. Brandt, *Int. J. Mod. Phys. B* **5**, 751 (1991).
³A. I. Larkin and Yu. N. Ovchinnikov, *Sov. Phys. JETP* **41**, 960 (1976).
⁴L. E. Musienko, I. M. Dmitrenko, and V. G. Volotskaya, *JETP Lett.* **31**, 567 (1980).
⁵W. Klein, R. P. Huebener, S. Gauss, and J. Parisi, *J. Low Temp. Phys.* **61**, 413 (1985).
⁶S. G. Doettinger, R. P. Huebener, R. Gerdemann, A. Kühle, S. Anders, T. G. Träuble, and J. C. Villegier, *Phys. Rev. Lett.* **73**, 1691 (1994).
⁷M. Tinkham, *Introduction to Superconductivity* (McGraw-Hill, New York, 1975).
⁸M. N. Kunchur, D. K. Christen, and J. M. Phillips, *Phys. Rev. Lett.* **70**, 998 (1993).
⁹R. Kleiner and P. Müller, *Phys. Rev. B* **49**, 1327 (1994).
¹⁰A. E. Koshelev and V. M. Vinokur, *Phys. Rev. Lett.* **73**, 3580 (1994).
¹¹R. Huber, M. Schneider, U. Wagner, and P. Ziemann, *J. Alloys Comp.* **195**, 255 (1993).
¹²P. Berberich, B. Utz, W. Prusseit, and H. Kinder, *Physica C* **219**, 497 (1994).
¹³M. Nahum, S. Verghese, P. L. Richards, and K. Char, *Appl. Phys. Lett.* **59**, 2034 (1991).
¹⁴C. D. Marshall, A. Tokmakoff, I. M. Fishman, C. B. Eom, Julia M. Phillips, and M. D. Fayer, *J. Appl. Phys.* **73**, 850 (1993).
¹⁵Y. Ando, H. Kubota, S. Tanaka, M. Aoyagi, H. Akoh, and S. Takada, *Phys. Rev. B* **47**, 5481 (1993).
¹⁶C. P. Bean, *Phys. Rev. Lett.* **8**, 250 (1962).
¹⁷Y. B. Kim, C. F. Hempstead, and A. R. Strnad, *Phys. Rev. Lett.* **9**, 306 (1962); P. W. Anderson, *ibid.* **9**, 309 (1962).
¹⁸F. Irie and K. Yamafuji, *J. Phys. Soc. Jpn.* **23**, 255 (1967).
¹⁹M. Xu, D. L. Shi, and F. Fox, *Phys. Rev. B* **42**, 10773 (1990).
²⁰J. L. Chen and T. J. Yang, *Physica C* **224**, 345 (1994).
²¹P. Fournier, M. Aubin, and M. A. R. LeBlanc, *Phys. Rev. B* **50**, 9548 (1994).
²²R. Griessen, Wen Hai-Hu, A. J. J. van Dalen, B. Dam, J. Rector, and H. G. Schnack, *Phys. Rev. Lett.* **72**, 1910 (1994).
²³K. A. Müller, M. Takashige, and J. G. Bednorz, *Phys. Rev. Lett.* **58**, 1143 (1987); J. Deak, L. F. Hou, P. Metcalf, and M. McElfresh, *Phys. Rev. B* **51**, 705 (1995).
²⁴Y. Yeshurun and A. P. Malozemoff, *Phys. Rev. Lett.* **60**, 2202 (1988); Y. W. Xu and M. Suenaga, *Phys. Rev. B* **43**, 5516 (1991).
²⁵M. A. Moore, *Phys. Rev. B* **39**, 136 (1989); H. R. Glyde, F. Lesage, and P. Findeisen, *ibid.* **46**, 9175 (1992).